P A U D W F A D T V

K M , B H , B F , B Q , *Member, IEEE*

Abstract*— We propose an ultrasound speckle filtering method for not only preserving various edge features but also filtering tissue-dependent complex speckle noises in ultrasound images. The key idea is to detect these various edges using a phase congruence-based edge significance measure called phase asymmetry (PAS), which is invariant to the intensity amplitude of edges and takes 0 in non-edge smooth regions and 1 at the idea step edge, while also taking intermediate values at slowly varying ramp edges. By leveraging the PAS metric in designing weighting coefficients to maintain a balance between fractional-order anisotropic diffusion and total variation (TV) filters in TV cost function, we propose a new fractional TV framework to not only achieve the best despeckling performance with ramp edge preservation but also reduce the staircase effect produced by integral-order filters. Then, we exploit the PAS metric in designing a new fractional-order diffusion coefficient to properly preserve low-contrast edges in diffusion filtering. Finally, different from fixed fractional-order diffusion filters, an adaptive fractional order is introduced based on the PAS metric to enhance various weak edges in the spatially transitional areas between objects. The proposed fractional TV model is minimized using the gradient descent method to obtain the final denoised image. The experimental results and real application of ultrasound breast image segmentation show that the proposed method outperforms other state-of-the-art ultrasound despeckling filters for both speckle reduction and feature preservation in terms of visual evaluation and quantitative indices. The best scores on feature similarity indices have achieved 0.867, 0.844 and 0.834 under three different levels of noise, while the best breast ultrasound segmentation accuracy in terms of the mean and median dice similarity coefficient are 96.25% and 96.15%, respectively.

***Index Terms*— Ultrasound despeckling, speckle noise, fractional-order diffusion filter, fractional-order TV filter, edge detection, phase congruency, phase asymmetry, image denoising.**

M M 13, 2019; O 16, 2019; N 8, 2019. D N 19, 2019; J 23, 2020. T N N S F C G 61271320, M E C F S J T U G YG2014MS29, T M C F S J T U G ZH2018ZDA19. T D. J C . *(Corresponding author: Binjie Qin.)*

K. M B. Q S B E , S J T U , S 200240, C (- : @ . .).
B. H D U M , S J T U A S P ' H , S I U M , S 200233, C .
B. F D B , E J S E C S , T U T D , R , TX 75080 USA.

T ://
D O I 10.1109/TIP.2019.2953361

I. INTRODUCTION

CURRENT [1], [2] [3], [4] - - . I - , - [5], [6] , ; , . T , [5] [7]. S [8], - [7]. F , - [9] 3D 2D [10]. T , - . H , - - , - , , [11]. T , - , . F - ( ) . E - [13], [14] , . V - , , - (NLM) . T F [14]

[15]
I , C et al. [16]
. M , (SBF) [17]
. H ,
. T NLM
. NLM
. C et al. [18]
B NLM (OBNLM)
-G . A
OBNLM Z et al. [19]
. R , Z et al. [20] -
(NLLRF) -
, -
. H , NLM
, [21].
I , P M
- (AD) -
[22],
(SRAD) [23] -
(DPAD) [24] AD
. T SRAD
, DPAD
-
. T
[25]
. U
, C et al. [16]
. U
,
[26] [27]
. H ,
-
,
. M ,
,
. T , B F [28]
- AD (FAD)
. N , -
.
R , F et al. [8]
-G (ADLG)
- . H , ADLG
. B AD
,

[29] - [30] - -
AD -
- ,
. H , -
-
.
E ,
, - - -
. T -
. A ,
, , ,
,
[31].
T ,
. T
[32] -
, O et al. [33]
. H ,
[2]
. C et al. [34]
. S
,
[35], -
[36], [37], [38], . H
,
,
.
T - ,
- [39], [40]
. I -
,
-
,
. M ,
-
- M et al. [41], [42].
T
, F
. A
- . T ,
, M . T -
M -P N [43]. W
[44] -
(PC)- (PS)
(PAS,
T I)

TABLE I
ACRONYMS

[redacted]	[redacted]

. I , . A , - - (AM-FM) [48] [50] , , [51], [40] [52]. T [53] 2D f R. T f_M: $f_M = (f, f_R) = (f, r_1 * f, r_2 * f)$, f_R R f, $r_1(x_1, x_2)$ $r_2(x_1, x_2)$ R , :

$$r_1(x_1, x_2) = \frac{-x_1}{2\pi\left(x_1^2 + x_2^2\right)^{3/2}}$$
$$r_2(x_1, x_2) = \frac{-x_2}{2\pi\left(x_1^2 + x_2^2\right)^{3/2}} \qquad (1)$$

S , f_M b. T f_M $f_M = (b * f, b * r_1 * f, b * r_2 * f) = (e_s, o_s)$, e_s o_s - - .

S b e_s o_s; C , C F [54]. I , 2D C :

$$C(w) = n_c\,|w|^a \quad (-s\,|w|)\,,\, a \geq 1 \qquad (2)$$

$w = (w_1, w_2)$, s , $n_c = \left(\frac{\pi\, 4^{a+1} s^{2a+1}}{\Gamma(2a+1)}\right)^{\frac{1}{2}}$, $\Gamma(\cdot)$, a . W $a = 1.58$, [39]. T , K [44] PAS . T , - PAS :

$$PA = \sum_s \frac{\lfloor |o_s| - |e_s| - T_s \rfloor}{\sqrt{e_s^2 + o_s^2} + \varepsilon} \qquad (3)$$

PA PAS , ε , T_s - , $\lfloor\cdot\rfloor$, s C . S , s , s ( ) .

F . 1 PAS . W PAS $s = 5$ $s = 10$. T PAS $s = 20$ $s = 25$, . T PAS $s = 15$. T , $s = 15$.

F . 1. E PAS . ( ) T ; PAS : ( ) $s = 5$, ( ) $s = 10$, ( ) $s = 15$, ( ) $s = 20$, ( ) $s = 25$.

PAS . T PAS 0 1, 0 (-) 1 ( ) . I , . A , PAS . D PAS , . F , PAS 1.

B. Fractional-Order Differential

T - - - - [47]. F $f(x) \in L^2(R)$, - :

$$D^\alpha f(x) = \frac{d^\alpha f(x)}{d x^\alpha} \qquad (4)$$

α . T F $D^\alpha f(x)$:

$$\begin{aligned} D^\alpha f(x) \overset{FT}{\Leftrightarrow} (\hat{D}^\alpha f)(w) &= (iw)^\alpha \hat{f}(w) \\ &= |w|^\alpha \quad \left[i\,\theta^\alpha(w)\right] \hat{f}(w) \\ &= |w|^\alpha \quad \left[\frac{\alpha\pi i}{2} \quad (w)\right] \hat{f}(w) \end{aligned} \qquad (5)$$

w , $(\cdot)$, $(iw)^\alpha = |w|^\alpha \quad \left[\frac{\alpha\pi i}{2} \quad (w)\right]$. A - , - α, F . 2. F F . 2, $0 < w < 1$, . N - , $w > 1$, , α . T - , - .

D - . A -

F . 2. T - .

, -

[47]. E

,

- . T

[46]. T ,

- α PAS

S . III-A .

C , -

: C , G -L

(G-L) R -L (R-L) [55], [56].

S G-L

, G-L

. A [57], α-

$f(x)$ G-L :

$$D^{\alpha} f(x) \overset{\Delta}{=} \lim_{h \to 0} \frac{1}{h^{\alpha}} \sum_{l=0}^{\left[\frac{d-c}{h}\right]} (-1)^{l} \binom{\alpha}{l} f(x - lh) \tag{6}$$

α , $[c, d]$ $f(x)$,

$\frac{d-c}{h}$ $[\frac{d-c}{h}]$, $\binom{\alpha}{l}$

:

$$\binom{\alpha}{l} = \frac{\Gamma(\alpha+1)}{\Gamma(l+1)\Gamma(\alpha-l+1)} \tag{7}$$

$\Gamma(n) = (n-1)!$.

C. Fractional-Order AD Filter and Fractional-Order TV Filter

T -

AD [22] :

$$\frac{\partial u}{\partial t} = div\left[c\left(|\nabla u|\right) \cdot \nabla u\right], \tag{8}$$

div , $|\nabla u|$

∇u, $c(\cdot)$

λ , ; λ , . T -. I , λ PSNR [60]. W λ 0.01 . R - , PAS :

$$\begin{cases} \varphi = (PA-1)^2 \\ \gamma = PA(2-PA) \end{cases} \tag{15}$$

PA PA . B , PA 0, FAD . W PA 1, FTV . B PA 1, FAD .

H , FAD - , . T - , PAS . T PAS . F , PAS . W $f(|\nabla^{\alpha} u|)$ $c(\cdot)$ (12). T :

$$c\left(\left|\nabla^{\alpha} u\right|, PA\right) = 1 / \left[1 + \frac{|\nabla^{\alpha} u| \cdot (1 + 254 \cdot PA)}{k_1^2}\right] \tag{16}$$

$k_1 = k_0 \, e^{-0.05(n_{iter}-1)}$ k (9). H , n_{iter} , k_0 .

G , . A S . II-B, - α PAS . S , - [46] :

$$\alpha = 1 + \quad _2\left(1 + PA^2\right) \tag{17}$$

PA PAS . T $\alpha \in (1,2)$. T PFDTV - .

I , PAS . A PAS , . A (17), PAS α . T PFDTV - , .

B. Numerical Solver

W E -L [61] (14). A u $E(u)$, $E(u)$. I , u . W 0, 0. T $\eta \in C^{\infty}(\Omega)$ e. D :

$$\begin{aligned} \Phi(e) &:= E(u + e\eta) \\ &= \int_{\Omega} \left[\varphi f\left(\left|\nabla^{\alpha}(u + e\eta)\right|\right) + \gamma \left|\nabla^{\alpha}(u + e\eta)\right|\right] dxdy \\ &\quad + \int_{\Omega} \left(\frac{\lambda}{2} |u + e\eta - u_0|^2\right) dxdy \end{aligned} \tag{18}$$

W $\Phi(e)$:

$$\begin{aligned} \Phi'(e) &= \frac{d}{de}\Phi(e) \\ &= \varphi \int_{\Omega} \Bigg(f'\left(\left|\nabla^{\alpha}(u+e\eta)\right|\right) \\ &\quad \times \frac{\nabla_x^{\alpha}(u+e\eta)\nabla_x^{\alpha}\eta + \nabla_y^{\alpha}(u+e\eta)\nabla_y^{\alpha}\eta}{\sqrt{\left(\nabla_x^{\alpha}(u+e\eta)\right)^2 + \left(\nabla_y^{\alpha}(u+e\eta)\right)^2}} \Bigg) dxdy \\ &\quad + \gamma \int_{\Omega} \left(\frac{\nabla_x^{\alpha}(u+e\eta)\nabla_x^{\alpha}\eta + \nabla_y^{\alpha}(u+e\eta)\nabla_y^{\alpha}\eta}{\sqrt{\left(\nabla_x^{\alpha}(u+e\eta)\right)^2 + \left(\nabla_y^{\alpha}(u+e\eta)\right)^2}} \right) dxdy \\ &\quad + \lambda \int_{\Omega} (u + e\eta - u_0)\eta \, dxdy, \end{aligned} \tag{19}$$

L $e = 0$, :

$$\begin{aligned} &\Phi'(0) \\ &= \varphi \int_{\Omega} \left(c\left(\left|\nabla^{\alpha} u\right|^2, PA^2\right) \left(\nabla_x^{\alpha} u \, \nabla_x^{\alpha} \eta + \nabla_y^{\alpha} u \, \nabla_y^{\alpha} \eta\right) \right) dxdy \\ &\quad + \gamma \int_{\Omega} \frac{\nabla_x^{\alpha} u \, \nabla_x^{\alpha} \eta + \nabla_y^{\alpha} u \, \nabla_y^{\alpha} \eta}{|\nabla^{\alpha} u|} dxdy \\ &\quad + \lambda \int_{\Omega} (u - u_0)\eta \, dxdy \end{aligned} \tag{20}$$

$|\nabla^{\alpha} u| = \sqrt{\left(\nabla_x^{\alpha} u\right)^2 + \left(\nabla_y^{\alpha} u\right)^2}$. A u,

$\Phi'(0) = 0$. T (20), :

$$\nabla_x^\alpha u \, \nabla_x^\alpha \eta + \nabla_y^\alpha u \, \nabla_y^\alpha \eta = \left(\left(\nabla_x^\alpha\right)^* \nabla_x^\alpha u + \left(\nabla_y^\alpha\right)^* \nabla_y^\alpha u \right) \eta \tag{21}$$

$\left(\nabla_x^\alpha\right)^*$ $\left(\nabla_y^\alpha\right)^*$ ∇_x^α ∇_y^α [62]. B , (20) :

$$\begin{aligned} &\Phi'(0) \\ &= \varphi \int_\Omega c\left(\left|\nabla^\alpha u\right|^2, PA^2\right)\left(\left(\nabla_x^\alpha\right)^* \nabla_x^\alpha u + \left(\nabla_y^\alpha\right)^* \nabla_y^\alpha u\right) \eta \quad dy \\ &\quad + \gamma \int_\Omega \frac{\left(\nabla_x^\alpha\right)^* \nabla_x^\alpha u + \left(\nabla_y^\alpha\right)^* \nabla_y^\alpha u}{\left|\nabla^\alpha u\right|} \eta \quad dy \\ &\quad + \lambda \int_\Omega (u - u_0)\, \eta \quad dy \end{aligned} \tag{22}$$

F $\eta \in C^\infty(\Omega)$, E -L :

$$\begin{aligned} &\varphi c\left(\left|\nabla^\alpha u\right|^2, PA^2\right)\left(\left(\nabla_x^\alpha\right)^* \nabla_x^\alpha u + \left(\nabla_y^\alpha\right)^* \nabla_y^\alpha u\right) \\ &\qquad + \gamma \frac{\left(\nabla_x^\alpha\right)^* \nabla_x^\alpha u + \left(\nabla_y^\alpha\right)^* \nabla_y^\alpha u}{\left|\nabla^\alpha u\right|} + \lambda (u - u_0) = 0 \end{aligned} \tag{23}$$

u . L ∇E $E(u)$; u $E(u)$ $\nabla E = 0$. T , ∇E :

$$\begin{aligned} \nabla E &= \varphi c(\left|\nabla^\alpha u\right|^2, PA^2)((\nabla_x^\alpha)^* \nabla_x^\alpha u + (\nabla_y^\alpha)^* \nabla_y^\alpha u) \\ &\quad + \gamma \frac{(\nabla_x^\alpha)^* \nabla_x^\alpha u + (\nabla_y^\alpha)^* \nabla_y^\alpha u}{\left|\nabla^\alpha u\right|} + \lambda(u - u_0) \end{aligned} \tag{24}$$

T u [63]. S , Δt $-\nabla E$, *i.e.*, $u^{n+1} = u^n + \Delta t(-\nabla E)$. F , u $E(u)$.

C. Numerical Algorithm

T (24) , G-L - . W u $X \times Y$, X Y . T , ∇^α, ∇_y^α, $\left(\nabla_x^\alpha\right)^*$ $\left(\nabla_y^\alpha\right)^*$, :

$$\begin{cases} \nabla_x^\alpha u_{i,j} = \sum_{l=0}^{j} (-1)^l \binom{\alpha}{l} u_{i,j-l} \\ \nabla_y^\alpha u_{i,j} = \sum_{l=0}^{i} (-1)^l \binom{\alpha}{l} u_{i-l,j} \end{cases} \tag{25}$$

$$\begin{cases} \left(\nabla_x^\alpha\right)^* u_{i,j} = \sum_{l=0}^{Y-1-j} (-1)^l \binom{\alpha}{l} u_{i,j+l} \\ \left(\nabla_y^\alpha\right)^* u_{i,j} = \sum_{l=0}^{X-1-i} (-1)^l \binom{\alpha}{l} u_{i+l,j} \end{cases} \tag{26}$$

Algorithm 1 PFDTV F -P D F

Input:

TABLE II

COMPARISON OF THE PSNR, MSSIM AND FSIM VALUES AMONG DIFFERENT FILTERS

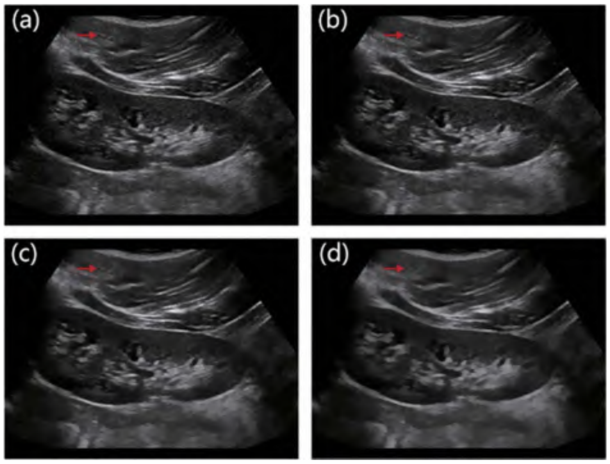

F . 4. E k_0. ( ) T ; ( ) $k_0 = 5$, ( ) $k_0 = 20$, ( ) $k_0 = 100$.

. T MSSIM . T FSIM PFDTV .

B. Clinical Image Experiment

S , . T , PFDTV . T .[3]

T . T , PFDTV . T : s, k_0 n_{iter}. A S II-A, s

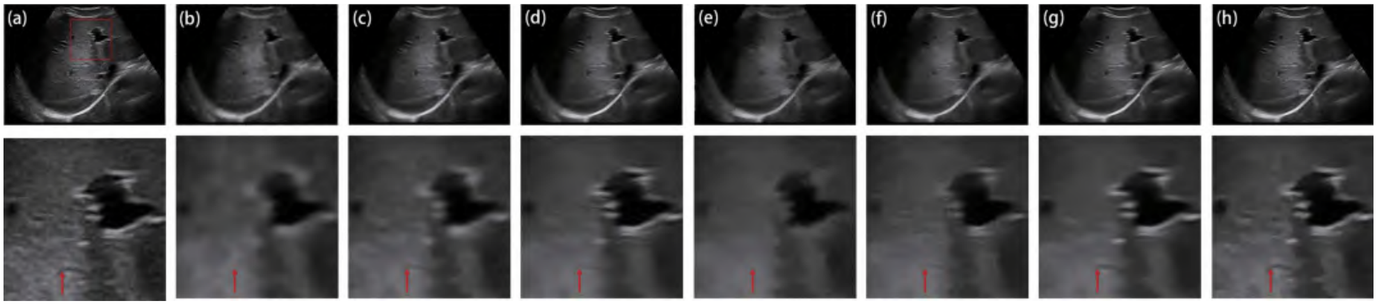

F . 6. D . ( ) T ; ( ) F , ( ) SRAD, ( ) OBNLM, ( ) SBF, ( ) ADLG, ( ) NLLRF, ( ) **PFDTV**.

F . 7. D . ( ) T ; ( ) F , ( ) SRAD, ( ) OBNLM, ( ) SBF, ( ) ADLG, ( ) NLLRF, ( ) **PFDTV**.

. S , F . 7, PFDTV . SRAD, OBNLM NLLRF . O . T

F . 8. D ( ). T ROI - , . ( ) T ; ( ) F , ( ) SRAD, ( ) OBNLM, ( ) SBF, ( ) ADLG, ( ) NLLRF, ( ) **PFDTV**.

, DSC JS - . A , HD HM . H , DSC JS, HD HM. T III T IV DSC, JS, HD HM BUS , . O , PFDTV DSC JS , HD HM , PFDTV .

T OBNLM, NLLRF PFDTV I (R) C (TM) CPU 2.71 GH 8 GB RAM. T F . 7( ) 225×300 86.54 . OBNLM 2.85 NLLRF 430.21 . A PFDTV

TABLE III

THE MEAN DSC, JS, HD AND HM VALUES FOR DIFFERENT SEGMENTATION RESULTS ON TEN BREAST ULTRASOUND IMAGES

	DSC(%)	JS(%)	HD	HM
Input	91.87	85.02	16.9933	3.3599
Frost	93.62	88.02	9.8418	2.1265
SRAD	94.02	90.52	8.2271	1.5781

(a) (b) (c) (d)

F . 9. M PFDTV . F ; . ( ) ( ) , ( ) , ( ) .

F . 10. T . Y : ; G : . ( ) T . D ( ) F , ( ) SRAD, ( ) OBNLM, ( ) SBF, ( ) ADLG, ( ) NLLRF, ( ) **PFDTV**.

TABLE IV

THE MEDIAN DSC, JS, HD AND HM VALUES FOR DIFFERENT SEGMENTATION RESULTS ON TEN BREAST ULTRASOUND IMAGES

- . I -
- - -
[2], ACVA
- G P -G
. T , -
[78], [79]
PFDTV
.
I -
[35], [76], [80] -
. M
, 3D [7], [81]
, -
. H , fi
.
T ,
/ - [82]
-
.
T *s*
-
. T [39]
. F
[38], [39] .
I ,
- TV FAD
FTV - -
. S
- TV -
-
.

ACKNOWLEDGEMENT

T -

[29] A. S. L H. M. P , A , *Measurement*, . 140, . 572 581, J . 2019.
[30] D. G , R. S. A , B. T , S - - , *IET Image Process.*, . 9, . 2, . 107 117, 2015.
[31] Z. Q , L. Y , W. L , A - , *Proc. BMVC*, 2011, . 73.
[32] V. B. S. P , R. P , G. S , K. P , M - - , *IEEE Trans. Image Process.*, . 28, . 12, . 6198 6210, D . 2019.
[33] N. O , M. G , S. A , A. B , B. N , R. B , O , *IEEE Trans. Pattern Anal. Mach. Intell.*, , : 10.1109/TPAMI.2019.2892134.
[34] R. C , R. S , L. M , H. B , A : R - , A . 2019, *arXiv:1904.10235*. [O]. A : :// . / /1904.10235
[35] V. K , A. F , K. E , J. A , F - , *Int. J. Comput. Vis.*, . 86, . 1, . 1 32, 2010.
[36] H. T , S. F , P. M , K , *IEEE Trans. Image Process.*, . 16, . 2, . 349 366, F . 2007.
[37] B. Q , Z. S , Z. Z , J. Z , Y. L , S - - , *Appl. Soft Comput.*, . 46, . 851 867, S . 2016.
[38] B. Q , Z. S , Z. F , Z. Z , Y. L , J. B , J - - , *IEEE Access*, . 6, . 1, . 330 343, 2018.
[39] L. Z , W. W , J. Q , K.-H. W , K.-S. C , P.-A. H , F - , *Signal Process.*, . 134, . 275 284, M 2017.
[40] A. B , D. B , Y. M , P - , *IEEE Trans. Inf. Technol. Biomed.*, . 15, . 1, . 138 147, J . 2011.
[41] M. C. M , J. R , D. C. B , R. O , M , *Nature*, . 324, . 6049, . 250 253, N . 1986.
[42] M. C. M R. A. O , F , *Pattern Recognit. Lett.*, . 6, . 5, . 303 313, D . 1987.
[43] M. M -P J. A. N , 2D+T , *Med. Image Anal.*, . 4, . 1, . 21 30, 2000.
[44] P. K , I , *J. Comput. Vis. Res.*, . 1, . 3, . 1 26, 1999.
[45] G.-Q. Z , W.-W. J , K.-L. L , Y.-P. Z , A 3-D , *IEEE Trans. Med. Imag.*, . 36, . 6, . 1250 1262, J . 2017.
[46] Q. Z , J. G , Z. W , K. L , A , *IEEE Trans. Geosci. Remote Sens.*, . 54, . 4, . 1905 1917, A . 2016.
[47] J. Y , L. T , S. Z , L. W , M. A. S , I , *IEEE Access*, . 5, . 12275 12285, 2017.
[48] V. M , P. R , M. S. P , M AM-FM - , *IEEE Trans. Image Process.*, . 19, . 5, . 1138 1152, M 2010.
[49] J. P. H , P. T , A. C. B , AM-FM : F , *Handbook of Image and Video Processing*. A , T N : E , 2005, . 377 395.
[50] M. C , T. O , V. P , T : A (,)9-6.8(.)-5[([44(5)-0.20TD-0.0205T [(T)-357.6(( ) ( )-)-10/)83.9( )29.8(23.2(3)-12.8784469.9( )500.-1.1142T2-0.0

[76] B. G , A. D , S. A , B. S. S , A. S , I F - - - , *Inf. Fusion*, . 55, . 220 244, M . 2020.
[77] C. A. N. S N. D. A. M , G - , *IEEE Trans. Image Process.*, . 28, . 1, . 216 226, J . 2019.
[78] Y. J , X. J , W. J , A , *J. Vis. Commun. Image Represent.*, . 65, D . 2019, A . . 102661, : 10.1016/ . .2019.102661.
[79] Y.-F. P *et al.*, A - - : F - - , *IEEE Trans. Image Process.*, . 27, . 3, . 1214 1229, M . 2018.
[80] F. Z *et al.*, R P X- - P , *Phys. Med. Biol.*, . 58, . 6, . 1739, 2013.
[81] R. J. G. S , R. C , Y. C. E , D , *Proc. IEEE*, , : 10.1109/ JPROC.2019.2932116.
[82] X. J , S. L , X. F , L. Z , FOCN : A , *Proc. IEEE Conf. Comput. Vis. Pattern Recognit.*, J . 2019, . 6054 6063.

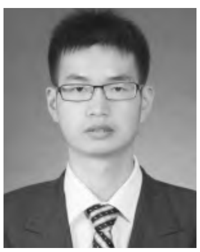

Kunqiang Mei B.S . - N U A A , N , M.S . S - J T U , S , C , 2016 2019, . H , , .

Bin Hu M.S. T U 1997, M.D.-P .D. S J T U , S , C , 2006. H , - . S S O P V U P C , C U M E - S U B C A A M S .

Baowei Fei M.S. P .D. C W R U , C , OH, USA. H P E J S E C S - , T U T D , R , TX, USA, D Q B L , D B C S .

Binjie Qin (M’07) M.S. N U S T - , N , 1999, P .D. S J T U , S , C , 2002. H L A P S L S B , S J T U . F 2012 2013, V P D C S , U C L , U.K. H A P S B E , S J T U . H - , , , , .